

Simultaneous analysis of stable and radiogenic strontium isotopes in reference materials, plants and modern tooth enamel

Danaé Guiserix^{a,*}, Emmanuelle Albalat^a, Henriette Ueckermann^b, Priyanka Davechand^c, Linda M. Iaccheri^c, Grant Bybee^c, Shaw Badenhorst^d, Vincent Balter^a

^a CNRS UMR 5276, LGLTPE, Univ. Lyon, ENS de Lyon, Univ. Lyon 1, 46 Allée d'Italie, 69342 Lyon Cedex 07, France

^b Department of Geology, University of Johannesburg, Auckland Park 2006, South Africa

^c School of Geosciences, University of the Witwatersrand, 1 Jan Smuts Avenue, Braamfontein, Johannesburg 2000, South Africa

^d Evolutionary Studies Institute, University of the Witwatersrand, Private Bag 3, Wits 2050, South Africa

ARTICLE INFO

Editor: Karen Johannesson

Keywords:

Non-traditional isotopes
Stable strontium isotopes
Radiogenic strontium isotopes
Trophic chain
Weaning

ABSTRACT

Radiogenic strontium isotopes ($^{87}\text{Sr}/^{86}\text{Sr}$) are a useful tool in forensics, ecology, bioarcheology and paleoanthropology allowing investigation of present and past migration and landscape use. The measurement of the $^{87}\text{Sr}/^{86}\text{Sr}$ ratio traditionally assumes a constant stable ($^{88}\text{Sr}/^{86}\text{Sr}$) isotope ratio. However, some studies indicate that these stable Sr isotopes may display mass-dependent fractionation, suggesting that the $^{88}\text{Sr}/^{86}\text{Sr}$ ratio may fingerprint previously unknown dietary and physiological information. Here we present a survey of the variability of $\delta^{88}\text{Sr}$ values, along with the $^{87}\text{Sr}/^{86}\text{Sr}$ ratios, in fourteen reference materials of geological and biological origin using MC-ICPMS. The measurements employ a simple sample-standard bracketing method and zirconium external correction. Comparisons with double-spiked $\delta^{88}\text{Sr}$ TIMS analyses show a very good agreement (0.014 ‰; $n = 10$). We then applied this method to explore the fractionation of the $^{88}\text{Sr}/^{86}\text{Sr}$ ratio in tooth enamel of mammals from two modern food-chains (Kruger National Park and Western Cape, South Africa), and from modern South African chacma baboon populations. Clear differences in the $\delta^{88}\text{Sr}$ values are observed between plants and teeth of herbivores (~ -0.26 ‰; $n = 5$), but the distinction between herbivores and carnivores requires further investigation. Variations between tooth enamel of young and adult baboons suggests that the $\delta^{88}\text{Sr}$ is a promising indicator of weaning behaviors. Our method implementation and preliminary results highlight the importance of coupled radiogenic and stable Sr isotope determination in extant and extinct vertebrates.

1. Introduction

There are four naturally occurring strontium (Sr) isotopes, all of which are stable (^{84}Sr , ^{86}Sr , ^{88}Sr , ^{87}Sr), but one, ^{87}Sr , is the radiogenic product of the β -decay radioactivity of rubidium-87 (^{87}Rb ; half-life = 48.8 Ga). Given that the atomic properties of Sr are similar to those of calcium (Ca), Sr is incorporated into the body as a Ca substitute, undergoing discrimination processes that lower the Sr/Ca ratio during metabolic processes involving Ca (Balter, 2004). Multi-collector inductively-coupled plasma mass spectrometers (MC-ICPMS) and thermal ionization mass spectrometers (TIMS), which are routinely used for the measurements of the $^{87}\text{Sr}/^{86}\text{Sr}$ ratio, induce an instrumental mass-bias during measurement that needs to be corrected, thus the true $^{86}\text{Sr}/^{88}\text{Sr}$ ratio is traditionally set at 0.1194 to correct the mass-bias on the $^{87}\text{Sr}/^{86}\text{Sr}$ ratio. The $^{87}\text{Sr}/^{86}\text{Sr}$ ratio in the body of an animal records

that of the soil/substrate on which the animal lives (Price et al., 2002; Lazzarini et al., 2021). By measuring the $^{87}\text{Sr}/^{86}\text{Sr}$ ratio in tissues forming at different periods of life, such as bone and tooth enamel, or within tooth enamel using laser ablation, it is possible to reconstruct the mobility and range of the animal, with reference to the Sr isotope ratio of the substrate (Knudson et al., 2004; Sillen and Balter, 2018).

However, with the improvement of MC-ICPMS precision in the last twenty years, variations of the $^{88}\text{Sr}/^{86}\text{Sr}$ ratio have been increasingly scrutinized in geological materials since the first measurement of that ratio in seawater (Fietzke and Eisenhauer, 2006). Variations of this ratio relative to the international standard NIST SRM-987 are expressed as $\delta^{88/86}\text{Sr}_{\text{SRM987}}$, defined as following:

$$\delta^{88/86}\text{Sr}_{\text{SRM987}} = \left(\frac{{}^{88}\text{Sr}/{}^{86}\text{Sr}_{\text{sample}}}{{}^{88}\text{Sr}/{}^{86}\text{Sr}_{\text{NIST SRM987}}} - 1 \right) \times 1000$$

* Corresponding author.

E-mail address: danae.guiserix@ens-lyon.fr (D. Guiserix).

The classical and shorter notation $\delta^{88}\text{Sr}$ will be used in the following text. There is only scarce data concerning the $\delta^{88}\text{Sr}$ value in biological materials. Recent studies suggest that stable Sr isotopes in bone and tooth enamel may be a good indicator of paleodietary range and trophic level (Knudson et al., 2010; Lewis et al., 2017; Brazier et al., 2020). Indeed, ^{86}Sr seems to be preferentially incorporated into biological system compared to ^{88}Sr . Analyses of plants show preferred uptake of ^{86}Sr relative to ^{88}Sr in the nutrient pathways leading to lighter isotopic signatures in leaves than in roots and soil (de Souza et al., 2010; Liu et al., 2016; Guibourdenche et al., 2020). Up trophic chains, the Sr isotope fractionation remains poorly studied, but it is already noticeable that all $\delta^{88}\text{Sr}$ values in plants are positive (de Souza et al., 2010; Liu et al., 2016; Hajj et al., 2017; Brazier et al., 2020), while all $\delta^{88}\text{Sr}$ values in terrestrial animals are negative (Knudson et al., 2010; Lewis et al., 2017; Brazier et al., 2020), relative to the SRM-987 standard. In a controlled feeding study on pigs, a shift of -0.32‰ from diet to dental enamel has been observed (Lewis et al., 2017), consistent with the plant data. Different methods have been developed in order to overcome instrumental mass bias during measurements of the $^{88}\text{Sr}/^{86}\text{Sr}$ and $^{87}\text{Sr}/^{86}\text{Sr}$ ratios. Analyses with a TIMS use a $^{84}\text{Sr}/^{86}\text{Sr}$ double spike to correct for the instrumental mass bias (Krabbenhöft et al., 2009; Neymark et al., 2014; Charlier et al., 2017; Lewis et al., 2017; Brazier et al., 2020) and is the method of reference to achieve the best precision (between 0.01 and 0.02 ‰ (Brazier et al., 2020)). Measurement method using a MC-ICPMS includes sample-standard bracketing method (SSB) (Fietzke and Eisenhauer, 2006; Ma et al., 2013) and correction using a zirconium (Zr) internal standard (Ohno and Hirata, 2007; Liu et al., 2012, 2016, 2017; Xu et al., 2020). Both methods can be used simultaneously (Irrgeher et al., 2013; Liu et al., 2017; Argentino et al., 2021).

A combination of these two methods is used in the present study and we test the procedure on fourteen reference materials with various mineral and biological matrices. The robustness and accuracy of this method was assessed in different laboratories. In South Africa sample preparation was done at the Wits Isotope Geoscience Laboratory (WIGL, University of the Witwatersrand, Johannesburg, South Africa), while the analytical measurements were done at the University of Johannesburg (UJ, Johannesburg, South Africa). Further work was achieved at the Laboratoire de géologie de Lyon (LGLTPE, Ecole Normale Supérieure de Lyon, France). In addition to the reference materials, we also measured the $^{88}\text{Sr}/^{86}\text{Sr}$ and $^{87}\text{Sr}/^{86}\text{Sr}$ ratios in animal and plant samples from extant ecosystems in South Africa to provide a first overview of the Sr stable isotope systematics in modern ecosystems and to challenge the possible use as a paleodietary indicator.

2. Material and methods

2.1. Reference material description

Eleven reference materials with known $^{88}\text{Sr}/^{86}\text{Sr}$ and $^{87}\text{Sr}/^{86}\text{Sr}$ ratios (biological matrix: SRM-1400, SRM-1486, BCR-380R, BCR-383 and SRM-1570a; geological matrix: JC-p1, UB-N, BHVO-2, BCR-1, and GS-N; seawater: IAPSO) and three reference materials with unknown $^{88}\text{Sr}/^{86}\text{Sr}$ and $^{87}\text{Sr}/^{86}\text{Sr}$ ratios (geological matrix: Granite GA, NBS-120c and SRM-915b) were analyzed in both labs. The descriptions of the standards are provided in Table 1. Reference material aliquots were weighed to reach around 5 μg of Sr.

2.2. Sample description

We also measure $^{88}\text{Sr}/^{86}\text{Sr}$ and $^{87}\text{Sr}/^{86}\text{Sr}$ ratios in two sets of modern samples. The first set of samples are from tooth enamel collected from modern chacma baboon (*Papio ursinus*) skulls provided by the Ditsong National Museum of Natural History (Pretoria, South Africa). Teeth were extracted from sixteen skulls of chacma baboons from a reserve in Calitzdorp (Western Cape, South Africa). Details for baboons and the geographical context are available in a previous study (Brand, 1994).

Table 1

Description of the reference materials analyzed in this study.

Reference material	Description	Sr ($\mu\text{g}\cdot\text{g}^{-1}$)
Animal		
BCR-380R	Whole milk powder	2.72
NIST SRM 1400	Cow bone ash powder	249
NIST SRM 1486	Cow bone meal powder	264
Vegetal		
BCR-383	Green bean powder	5.26
NIST SRM 1570a	Spinach powder	55
Carbonate		
JC-p1	Coral powder (<i>Porites</i> sp.)	6896
NIST SRM 915b	Calcium carbonate	150
Sea water		
IAPSO	North Atlantic sea water	7.9
Crustal and mantle rocks		
UB-N	Serpentine powder	9
BHVO-2	Basalt powder	389
BCR-1	Basalt powder	330
GS-N	Granite powder	570
Granite GA	Granite powder	310
NIST NBS 120c	Phosphate rock powder	840

The list of sampled individuals is presented in Table S1. The first molar of the upper jaw was sampled in 4 adults (over 6 years old) and 3 sub-adults (around 3 years old). Deciduous teeth (milk incisor, molar and canine) from 8 sub-adult baboons and the third molar from an adult were also sampled. All the teeth were washed with distilled water before drilling and the surfaces were cleaned with an abrasive drill bit. Sampling was located in the mesio- or distobuccal cusps of the teeth, and drilled using a bit diameter of 0.8 mm. Only the enamel was sampled to avoid contamination with dentine. Between 5 and 10 mg of powder was recovered. This set of material has been analyzed at UJ, using the WIGL-UJ method. The second set of samples consists in tooth enamel of herbivores and carnivores from the Kruger National Park (KNP) and Western Cape (WC), in South Africa. Details for sex, age and geographical context of these specimens are given in Table S2. The teeth were cleaned with distilled water before sampling. Plant residues trapped in the dentition of herbivorous mammals were also collected. The samples were stored at the Ditsong National Museum of Natural History (Pretoria, South Africa). They were prepared and analyzed at the LGLTPE, using the LGLTPE-2 analytical method. Around 5 mg of enamel powder was sampled, and the same quantity was taken from plant residues.

2.3. Sample digestion

2.3.1. WIGL

All sample preparation procedures were carried out in a Class 100 clean room under laminar flow hoods. Organics present in biological samples were removed via an oxidative digestion procedure. Thus 2 mL of concentrated HNO_3 (14 M) and 0.5 mL of H_2O_2 (30%) were added to SRM-1400 and SRM-1486, but also to evaporated IAPSO and baboon tooth enamel. Beakers were then left on a hotplate for three days at 110 °C. They were opened at regular 10 min intervals during the first hours to allow degassing. The BHVO-2 standard was dissolved using 2 mL of concentrated HNO_3 (14 M) and 1 mL concentrated HF. The closed beakers were left on a hotplate (110 °C) for 48 h. After complete dissolution all the samples were dried down and subsequently taken up with 1 mL of HNO_3 (3 M).

2.3.2. LGLTPE

Sample preparation procedures at the LGLTPE were carried out in a

Table 2

Ion exchange protocols for the chromatographic separation of Sr.

Lab	WIGL	LGLTPE
Wash	4 mL 0.5 M HNO ₃	4 mL 0.5 M HNO ₃
Conditioning	2.5 mL 3 M HNO ₃	2.5 mL 3 M HNO ₃
Load sample	1 mL 3 M HNO ₃	1 mL 3 M HNO ₃
Matrix elution	2.5 mL 3 M HNO ₃	3.5 mL 3 M HNO ₃
Sr elution	16 mL 0.5 M HNO ₃	7 mL 0.005 M HNO ₃

clean room under laminar flow hoods. All the acids used were purified twice by sub-boiling distillation. As at the WIGL, 4 mL concentrated HNO₃ (15 M) and 1 mL H₂O₂ (30%) were added to standards containing organics (i.e., BCR-383, BCR-380R, SRM-1486, SRM-1400 and SRM-1570a), but also to IAPSO and JC-p1, and closed beakers were left on a hotplate (110 °C) for 48 h. They were unscrewed regularly to allow degassing. Tooth enamel samples and plant residues from the KNP and WC were dissolved using the same protocol. The SRM-915b and NBS-120c standards were dissolved in 1 mL concentrated HNO₃ (15 M) and centrifuged to remove potential silicate particles. All rock samples (i.e., UB-N, BHVO-2, BCR-1, GS-N and Granite GA) were digested using 2 mL concentrated HNO₃ (15 M) and 1 mL concentrated HF. Closed beakers were left on the hotplate (110 °C) for 48 h and evaporated to dryness, taken up with 6 N HCl and a few drops of HClO₄ and evaporated on a hotplate (120 °C) to eliminate fluorides. This last step was repeated until all fluorides were dissolved. After, digestion all the samples were dried down and redissolved in 1 mL of 3 M HNO₃.

2.4. Sample preparation and instrumentation

2.4.1. WIGL

Isotopic measurements of Sr in biological and geological samples require the separation of Sr from the matrix with a special attention to avoid any isobaric interference with ⁸⁷Rb and Zr contamination. Strontium must be recovered quantitatively after the chromatographic separation to ensure the absence of any chemical isotopic mass fractionation during matrix and Sr elutions. The column chemistry protocol set up at WIGL was inspired by that of Tacail et al. (Tacail et al., 2014) and De Muynck et al. (De Muynck et al., 2009). Both protocols use the Sr specTM resin (TrisKem International). 300 µL of Sr specTM resin is loaded into 2 mL polypropylene columns. The elution protocol is given in Table 2. The resin is discarded after a single use.

Table 3

Instrument settings and data acquisition parameters for MC-ICP-MS analysis, and main differences between the three measurement methods.

Method	UJ	LGLTPE-1	LGLTPE-2
Element (+internal standard)	Sr(+Zr)	Sr(+Zr)	Sr(+Zr)
MC-ICP-MS	Nu Plasma II	Nu Plasma 500	Nu Plasma 500
RF power (W)	1300	1350	1350
Plasma condition	wet, cyclonic spray chamber	idem	idem
Coolant Ar flow (<i>L. min</i> ⁻¹)	13.00	13.00	13.5
Auxiliary Ar flow (<i>L. min</i> ⁻¹)	0.80	1.46	1.80
Nebulizer Ar flow (<i>L. min</i> ⁻¹)	34.50	37.9	35.1
Mass resolution	300	300	300
Cup configuration	H6: ⁹¹ Zr; H5: ⁹⁰ Zr H1: ⁸⁸ Sr; L1: ⁸⁷ Sr L3: ⁸⁶ Sr; L5: ⁸⁵ Rb L6: ⁸³ Kr; L7: ⁸² Kr ⁸⁸ Sr 0.5 ppm: 8 V	H6: ⁹¹ Zr; H5: ⁹⁰ Zr H2: ⁸⁸ Sr; Ax: ⁸⁷ Sr L2: ⁸⁶ Sr; L3: ⁸⁵ Rb L4: ⁸⁴ Sr; L5: ⁸³ Kr ⁸⁸ Sr 0.3 ppm: 8 V	H6: ⁹² Zr; H5: ⁹¹ Zr H4: ⁹⁰ Zr; Ax: ⁸⁸ Sr L2: ⁸⁷ Sr; L3: ⁸⁶ Sr L4: ⁸⁵ Rb; L5: ⁸⁴ Sr ⁸⁸ Sr 0.3 ppm: 8 V
Sensitivity			
Integration time (s)	10	10	10
Cycles	40	40	20
Isotope ratio used for mass bias correction of ⁸⁸ Sr/ ⁸⁶ Sr	⁹¹ Zr/ ⁹⁰ Zr	⁹¹ Zr/ ⁹⁰ Zr	⁹² Zr/ ⁹⁰ Zr and ⁹¹ Zr/ ⁹⁰ Zr
Baselines	On-peak zero	Deflected beam	On-peak zero
Blank signal	2.7*10 ⁻³ V	3.5*10 ⁻³ V	3.5*10 ⁻³ V
Kr interference correction	None	Yes	None
Rb interference correction	Yes	Yes	Yes

2.4.2. UJ

The isotopic analyses were performed on a Nu Plasma II (Nu Instrument) MC-ICPMS at UJ. The SRM-987 was used as the isotopic reference standard for Sr. On the day of the analysis session, samples and standards were diluted with 0.05 M HNO₃ to reach a concentration of 500 µg.L⁻¹, leading to a typical intensity of 8 V in the H1 collector (⁸⁸Sr). A high purity Zr solution (Alfa Aesar, 1000 ppm) was diluted and added to the standard and sample solutions at 500 µg.L⁻¹. The true ratio of ⁹¹Zr/⁹⁰Zr is 0.218126 according to the commission on isotopic abundances IUPAC (Meija et al., 2016). Measurements were carried out in static mode and a single measurement consisted of one block of 40 cycles with an integration time of 10 s. Daily calibration was performed to optimize operating conditions for maximum Sr and Zr signal stability, which was monitored with repeated measurements on SRM-987. The instrument settings are given in Table 3.

2.4.2.1. Interference correction. Krypton (Kr) contamination of argon (Ar) gas may interfere with ⁸⁶Sr. Measurement background was determined at the start of each measurement session by analyzing a 0.05 M HNO₃ laboratory blank. The on-peak background intensities were subtracted from the measurement signals during measurement, correcting for possible Kr interference.

To calculate the ⁸⁷Sr/⁸⁶Sr values, the isobaric interference of ⁸⁷Rb on ⁸⁷Sr was corrected following the equation:

$$^{87}\text{Rb} = \text{Meas}(^{85}\text{Rb}) \times \text{Ref}(^{87}\text{Rb}/^{85}\text{Rb}) \times \left(\frac{M(^{87}\text{Rb})}{M(^{85}\text{Rb})} \right)^{\text{Fract}_s} \quad (1)$$

$$^{87}\text{Sr} = \text{Meas}(^{87}\text{Sr}) - ^{87}\text{Rb} \quad (2)$$

With $\text{Meas}(^{85}\text{Rb})$ and $\text{Meas}(^{87}\text{Sr})$ being the measured intensity at mass 85 and 87, respectively, and $M(^{87}\text{Rb})$ and $M(^{85}\text{Rb})$ corresponding to Rb isotopic masses. $\text{Ref}(^{87}\text{Rb}/^{85}\text{Rb})$ is the natural abundance ratio extracted from the latest IUPAC report (0.3856, (Meija et al., 2016)). Fract_s is the fractionation factor defined as in Eq. (3) that can be used to correct for Rb interferences as long as the Rb concentration in the sample is small (Ehrlich et al., 2001). The average measured intensity of mass 85 in the samples was 2×10^{-05} V, which is negligible compared to the intensity measured on mass 87 (0.7 V).

2.4.2.2. Normalization of ⁸⁷Sr/⁸⁶Sr ratio. The ⁸⁷Sr/⁸⁶Sr ratio was obtained according to classic calculations (Marisa Almeida and D. Vasconcelos, 2001). The instrumental mass bias is evaluated by the

fractionation factor $Fract_{Sr}$, calculated using Russel's exponential law (Russell et al., 1978):

$$Fract_{Sr} = \frac{\ln\left(\frac{True(^{86}Sr/^{88}Sr)}{Meas(^{86}Sr/^{88}Sr)}\right)}{\ln\left(\frac{M(^{86}Sr)}{M(^{88}Sr)}\right)} \quad (3)$$

$M(^{88}Sr)$ and $M(^{86}Sr)$ correspond to Sr isotopic masses and $True(^{86}Sr/^{88}Sr)$ equals 0.1194 (Meija et al., 2016). This fractionation factor can then be used to normalize the $^{87}Sr/^{86}Sr$ ratio:

$$Norm(^{87}Sr/^{86}Sr) = Meas(^{87}Sr/^{86}Sr) \times \left(\frac{M(^{87}Sr)}{M(^{86}Sr)}\right)^{Fract_{Sr}} \quad (4)$$

However, the mass bias may change during the analytical session. Thus, a sample-standard bracketing method (SSB) was applied to take these variations into account, using the equation:

$$\left(^{87}Sr/^{86}Sr\right)_{sample} = Norm(^{87}Sr/^{86}Sr)_{sample} \times \frac{Ref(^{87}Sr/^{86}Sr)_{SRM987} \times 2}{Norm(^{87}Sr/^{86}Sr)_{stdA} + Norm(^{87}Sr/^{86}Sr)_{stdB}} \quad (5)$$

With $Norm(^{87}Sr/^{86}Sr)_{std}$ being the measured and normalized $^{87}Sr/^{86}Sr$ ratios of the previous (A) and following (B) standards. $Ref(^{87}Sr/^{86}Sr)_{SRM987}$ is the "true" $^{87}Sr/^{86}Sr$ value of the NIST SRM-987, set at 0.71024. Although NIST certifies the SRM-987 reference material $^{87}Sr/^{86}Sr$ value at 0.71034 ± 0.00026 , previous studies have rather been measuring and using a value of 0.71024, which falls inside the uncertainties of the certified value. This difference may be explained using 0.1194 as the true $^{86}Sr/^{88}Sr$, instead of the true value of this standard (0.119352). For the sake of comparison with other studies (e.g. Weber et al., 2018; Brazier et al., 2020), it was decided to use in the present study a SRM-987 $^{87}Sr/^{86}Sr$ value of 0.71024 as the bracketing standard value.

As the measurement method proposed here allows the measurements of the stable $^{88}Sr/^{86}Sr$ ratio corrected from the mass bias and the normalized radiogenic $^{87}Sr/^{86}Sr$ ratio simultaneously, it is possible to use the Zr-corrected $^{86}Sr/^{88}Sr$ ratio of a sample to normalize its $^{87}Sr/^{86}Sr$ ratio. However, the $^{87}Sr/^{86}Sr$ value in a biological sample obtained after normalization to a constant $^{86}Sr/^{88}Sr$ ratio of 0.1194 can solely correspond to the initial $^{87}Sr/^{86}Sr$ ratio i.e., that of the substrate, which depends ultimately on ^{87}Rb radioactive disintegration. This constitutes the methodological ground on which are based provenance and mobility studies. Taking these considerations into account and for the sake of comparison with previous work, in this study we decided to present only the $^{87}Sr/^{86}Sr$ ratio normalized with a constant $^{86}Sr/^{88}Sr$ ratio of 0.1194. A comparison of those two corrections through three analytical sessions can be found in Figs. S1 (Supplementary material) showing, as expected, a strong correlation with a 1:1 slope.

2.4.2.3. Correction of the $^{88}Sr/^{86}Sr$ ratio. Given that Zr and Sr have very similar masses, instrumental mass fractionation does not vary independently for both elements (Maréchal et al., 1999). Therefore, the Zr fractionation factor can then be used to correct $^{88}Sr/^{86}Sr$ using Russel's exponential law (Russell et al., 1978). The measured $^{91}Zr/^{90}Zr$ ratio is used to calculate the fractionation factor of the instrument ($Fract_{Zr}$) using the equation:

$$Fract_{Zr} = \frac{\ln\left(\frac{True(^{91}Zr/^{90}Zr)}{Meas(^{91}Zr/^{90}Zr)}\right)}{\ln\left(\frac{M(^{91}Zr)}{M(^{90}Zr)}\right)} \quad (6)$$

With $M(^{91}Zr)$ and $M(^{90}Zr)$ corresponding to Zr isotopes isotopic masses. The stable isotopic composition of Sr is then corrected using the equation:

$$Corr(^{88}Sr/^{86}Sr) = Meas(^{88}Sr/^{86}Sr) \times \left(\frac{M(^{88}Sr)}{M(^{86}Sr)}\right)^{Fract_{Zr}} \quad (7)$$

We also apply the sample-standard bracketing method (SSB) to correct for the instrumental mass-bias variations during the measurement session. The sample $\delta^{88}Sr$ value is calculated using the $^{88}Sr/^{86}Sr$ ratio averaged from the previous (A) and the following (B) standard:

$$\delta^{88}Sr = \left(\frac{Corr(^{88}Sr/^{86}Sr)_{sample} \times 2}{Corr(^{88}Sr/^{86}Sr)_{stdA} + Corr(^{88}Sr/^{86}Sr)_{stdB}} - 1\right) \times 1000 \quad (8)$$

This standard must have known Sr isotopic composition. Special care was given to closely match the concentration between the bracketing standard (SRM-987) and the samples (Ma et al., 2013; Liu et al., 2016). The co-variation between Sr and Zr can be observed in Figs. S2 and S3, showing the drift of the non-corrected $^{92}Zr/^{90}Zr$ and $^{88}Sr/^{86}Sr$ ratios in SRM-987 through an analytical session.

2.4.3. LGLTPE

Strontium was isolated from the matrix using a protocol similar to that set-up at WIGL with identical resin volume and size column, however the acid molarity for the Sr elution was slightly modified to reduce acid consumption. As shown in Table 2, Sr is eluted with 7 mL of 0.005 M HNO₃. A small aliquot (15 µL) was saved before and after the elution protocol for the quantitative determination of Sr and other trace element concentrations.

The measurement of Sr, Rb and Zr concentrations was performed on a quadrupole ICPMS (Thermo Scientific, iCap-Q) using the ^{85}Rb , ^{88}Sr and ^{90}Zr masses. Aliquots were diluted in 5 mL of 0.5 M HNO₃ with 2 µg.L⁻¹ rhodium (Rh) as an internal standard. Strontium recovery from the chromatographic separation was found to be $95.5 \pm 6\%$ (2SD, n = 24), suggesting quantitative yields and therefore absence of any mass-dependent fractionation. The low amount of Sr in procedural blanks (between 1 and 4 ng) was typically 0.04% of total Sr in the samples. After the chromatographic separation of Sr, the Sr/Zr ratio was >100 on average.

Isotopic analyses were performed on a Nu Plasma 500 MC-ICP-MS (Nu Instruments). On the day of the measurement session, samples and standards were diluted with 0.05 M HNO₃ to reach a Sr concentration corresponding to an intensity of 8 V in the H2 collector (^{88}Sr) (usually 250 or 300 µg.L⁻¹). The solutions were then doped with a high purity Zr solution (Alfa Aesar) to reach a $^{90}Zr/^{88}Sr$ close to unity. Measurements were carried out in static, multi collection mode and one single measurement consisted in one block of 40 cycles with an

integration time of 10 s. Electronic zero by ESA deflection were subtracted online on each measurement. Krypton possible contribution was monitored by measuring the intensity at mass 83 (^{83}Kr) and subtracting its influence on mass 86:

$$^{86}\text{Kr} = \text{Meas}(^{83}\text{Kr}) \times \text{Ref}\left(^{86}\text{Kr}/^{83}\text{Kr}\right) \quad (9)$$

$$^{86}\text{Sr} = \text{Meas}(^{86}\text{Sr}) - ^{86}\text{Kr} \quad (10)$$

With $M(^{86}\text{Kr})$ and $M(^{83}\text{Kr})$ corresponding to Kr isotopic masses. $\text{Ref}(^{86}\text{Kr}/^{83}\text{Kr})$ (1.50) is the ratio of Kr isotopes natural abundances extracted from the latest IUPAC report (Meija et al., 2016). The isobaric interference of ^{87}Rb on ^{87}Sr was corrected using Eqs. (1) and (2). The typical intensity on mass 85 (^{85}Rb) for the samples was 2×10^{-4} V which is low enough to use the correction, with a measured intensity of 0.7 V on mass 87. The $^{87}\text{Sr}/^{86}\text{Sr}$ ratio was normalized using Eqs. (3) and (4) and the instrumental induced mass-bias on $^{88}\text{Sr}/^{86}\text{Sr}$ was corrected using Eqs. (6) and (7). SSB was also applied using Eq. (8). This analytical method is indicated as LGLTPE-1.

A second analytical method was tested at LGLTPE, indicated as LGLTPE-2 in Table 3. This method used an on-peak baseline measurement with 10 s integration time prior to each measurement session using a 0.05 M HNO_3 blank. The measured intensities were then subtracted on line during the analytical sequence for all the samples and standards. Thus, the Kr correction became unnecessary and Eqs. (9) and (10) were not used. The collector configuration of the LGLTPE-2 method (Table 3) allowed the measurement of both $^{91}\text{Zr}/^{90}\text{Zr}$ and $^{92}\text{Zr}/^{90}\text{Zr}$ ratios. Thus the $^{88}\text{Sr}/^{86}\text{Sr}$ ratio could be corrected for mass bias using the $^{91}\text{Zr}/^{90}\text{Zr}$ and $^{92}\text{Zr}/^{90}\text{Zr}$ ratios with Eqs. (6) and (7), using $\text{True}(^{92}\text{Zr}/^{90}\text{Zr})$ of 0.333243 (Meija et al., 2016). It was observed by Liu and collaborators that best fit occurred between the mass bias affecting $^{92}\text{Zr}/^{90}\text{Zr}$ and $^{88}\text{Sr}/^{86}\text{Sr}$ ratios, compared to that affecting $^{91}\text{Zr}/^{90}\text{Zr}$ (Liu et al., 2012). These authors also find a better precision when using the $^{92}\text{Zr}/^{90}\text{Zr}$ ratio. In the present study, both corrections were compared. Measurements giving $\delta^{88}\text{Sr}$ values with differences higher than 0.05 ‰ between the two corrections were not considered. The samples $\delta^{88}\text{Sr}$ values given here with the LGLTPE-2 method are the $\delta^{88}\text{Sr}$ values corrected with the $^{92}\text{Zr}/^{90}\text{Zr}$ ratio. SSB was also applied using Eq. (8). Specificities of each method are summarized in Table 3.

2.5. U ($k = 2$) expanded uncertainties

The measurement uncertainties in this work regarding certified reference materials are given as expanded uncertainties (U) to compare with other studies. The measurement uncertainties were calculated by multiplying the combined uncertainty $u_c(y)$ of isotopic ratios by a coverage factor k such that $U = ku_c(y)$. Here $k = 2$, which corresponds to a level of confidence of 95%. The calculation of the combined uncertainty $u_c(y)$ of a δ value involves the uncertainties of the isotopic ratios of the sample and those of the bracketing standards. The full description of the calculation is presented in Sullivan et al. (Sullivan et al., 2020), and the final equation is given here for a symbolic rA/a isotope ratio:

$$u^2(r^{A/a}) = \left(\frac{1}{r_{std}^{A/a}}\right)^2 \times u^2(r_{std}^{A/a}) + \left(-\frac{r_{spl}^{A/a}}{(r_{std}^{A/a})^2}\right)^2 \times u^2(r_{spl}^{A/a}) \quad (11)$$

With std and spl corresponding to the standard and the sample, respectively, and $u(r)$ the standard uncertainty for the measured ratio, which can be estimated by using the standard deviation calculated from the different blocks corresponding to one block of measurement.

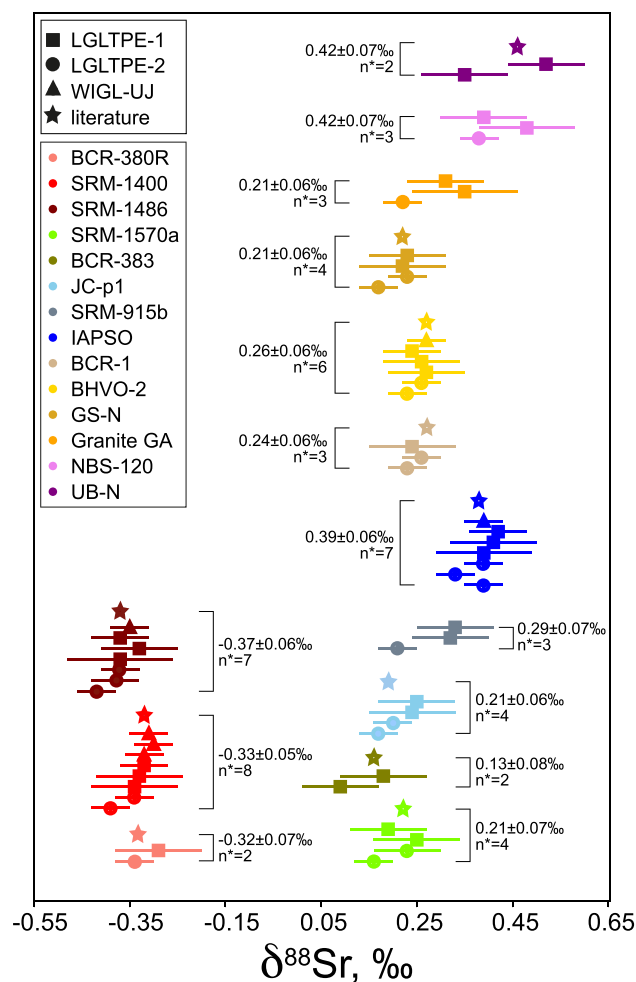


Fig. 1. $\delta^{88}\text{Sr}$ values for the reference materials measured in the WIGL-UJ and in the LGLTPE; Error associated to the mean value is the mean of U ($k = 2$) for each aliquot digested and processed according to the chromatographic procedure. The n^* value corresponds to the number of these aliquots. A mean of literature values is presented, all references used for the compilation are presented in Table S2.

3. Results

3.1. Reference materials

Sample-standard bracketing and the Sr correction methods described produced an $^{87}\text{Sr}/^{86}\text{Sr}$ ratio for SRM-987 of 0.71023 ± 0.00003 (U , $k = 2$, $n = 47$) at UJ, 0.71037 ± 0.00005 (U , $k = 2$, $n = 152$) for LGLTPE-1 and 0.71026 ± 0.00004 (U , $k = 2$, $n = 284$) for LGLTPE-2 (note again that the commonly used $^{87}\text{Sr}/^{86}\text{Sr}$ value is 0.71024 ± 0.00026 (McArthur et al., 2001; Weber et al., 2018; Brazier et al., 2020), while the certified value is 0.71034 ± 0.00026). Using the sample-standard bracketing and Zr correction methods, the corresponding SRM-987 $\delta^{88}\text{Sr}$ values are -0.003 ± 0.039 ‰ (U , $k = 2$, $n = 47$) at UJ, 0.001 ± 0.094 ‰ (U , $k = 2$, $n = 152$) for LGLTPE-1 and -0.001 ± 0.039 ‰ (U , $k = 2$, $n = 284$) for LGLTPE-2. The $\delta^{88}\text{Sr}$ results for the SRM-987 are summarized in Fig. S4. The analytical uncertainties in the LGLTPE show a clear improvement when using the LGLTPE-2 method. All the uncertainties are comparable with those measured by TIMS i.e. between 0.026 and 0.074 ‰, U , $k = 2$ (Brazier et al., 2020).

The $\delta^{88}\text{Sr}$ values of the fourteen reference materials are presented in Fig. 1 and compared with the literature values in Table S3. All literature values used for compilation are presented in Table S4. For the sake of

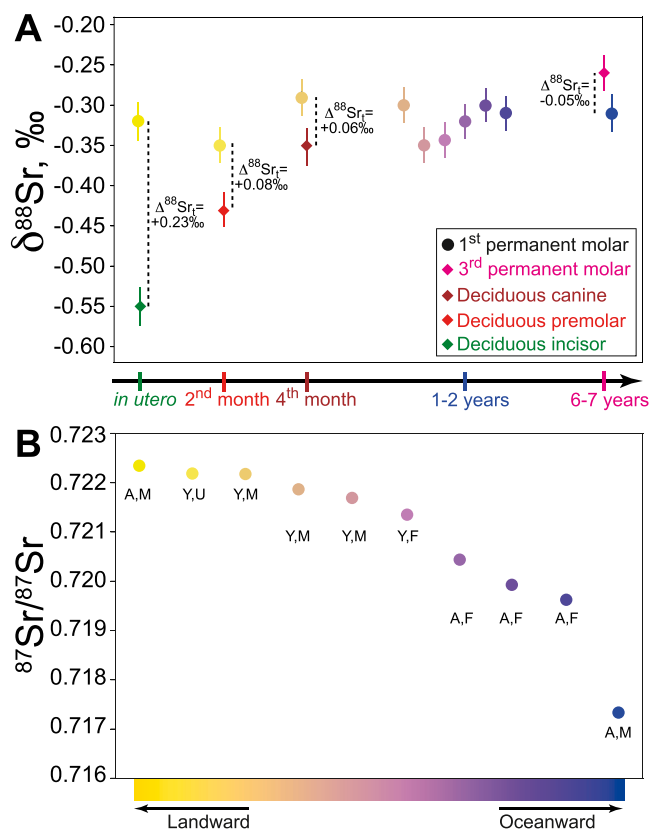


Fig. 2. A $\delta^{88}\text{Sr}$ results of the set of various teeth from the baboon skulls with their erupting order (note that for specimen with both deciduous tooth and 1st permanent molar analyzed, the result for the 1st permanent molar is not presented according to the timeline). Error bars are the 2SD calculated from repeated measurements of the SRM1400 during the same analytical session (0.02 ‰; 2SD; $n = 4$); $\Delta^{88}\text{Sr}_i$ is defined for a given specimen as the difference between $\delta^{88}\text{Sr}$ value in the first molar and $\delta^{88}\text{Sr}$ value in another tooth. B $^{87}\text{Sr}/^{86}\text{Sr}$ results for 10 baboon specimens; A = adult, Y = young, F = female, M = male, U = unknown sex; The color gradient for 1st molars identifies individuals in panel 2A and 2B.

visibility, only some of them are presented in Table S3.

For all standards except UB-N, the results from WIGL-UJ, LGLTPE-1 and LGLTPE-2 are identical within uncertainties. There is a good accuracy with literature values, even for less studied materials such as SRM-1400, SRM-1486, BCR-380R, BCR-383, SRM-1570a, BCR-1 and GS-N. The U ($k = 2$) uncertainties calculated in the present study range between 0.04 and 0.09 ‰. The measured values for UB-N are highly variable, and this variability can be found in the literature, as Brazier et al. (Brazier et al., 2020) and Ma et al. (Ma et al., 2013) are each finding different $\delta^{88}\text{Sr}$ values (0.389 ‰ and 0.539 ‰ respectively), suggesting that UB-N is a heterogeneous material.

Radiogenic Sr results for the fourteen reference materials are presented and compared to literature values in Table S5 and all literature values used for compilation are presented in Table S4. For all samples, the results of the present study are in good agreement with referenced values. The expanded uncertainty U ($k = 2$) on the $^{87}\text{Sr}/^{86}\text{Sr}$ ratio ranges between 3×10^{-5} and 6×10^{-5} , which is slightly higher than that achieved by TIMS (2×10^{-5} , (Brazier et al., 2020)).

3.2. Tooth enamel samples

The $\delta^{88}\text{Sr}$ values and $^{87}\text{Sr}/^{86}\text{Sr}$ ratios of baboon teeth are given in Table S1. All the samples from baboon teeth were analyzed only once, using the WIGL-UJ method. The mean $\delta^{88}\text{Sr}$ value for all first molars of

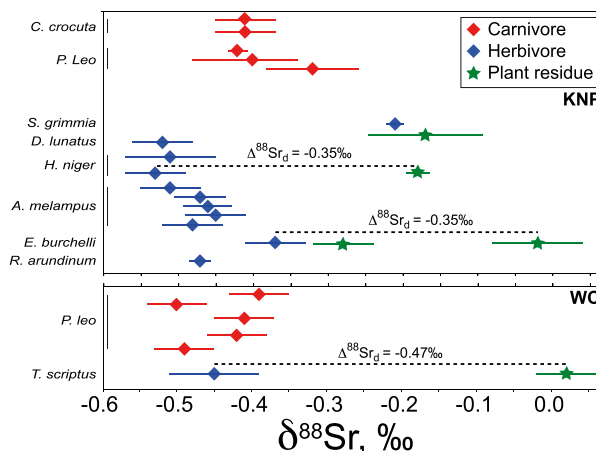


Fig. 3. $\delta^{88}\text{Sr}$ values for carnivores, herbivores and plants in KNP and WC; A dashed line links teeth and associated plant residues; The corresponding Sr isotope fractionation value ($\Delta^{88}\text{Sr}_i$) is given; Errors bars are 2SD calculated on repeated measurements of the same sample.

adult baboons is -0.31 ‰. Males (-0.30 ± 0.01 ‰, 2SD, $n = 2$) and females (-0.31 ± 0.02 ‰, 2SD, $n = 3$) have similar $\delta^{88}\text{Sr}$ values. The mean $\delta^{88}\text{Sr}$ value of all the first molars (adult and young specimens) is -0.32 ± 0.06 ‰ (2SD, $n = 10$). The three deciduous teeth $\delta^{88}\text{Sr}$ values are -0.55 ‰ (deciduous incisor), -0.43 ‰ (deciduous premolar), and -0.35 ‰ (deciduous canine). These are significantly lower than first molars $\delta^{88}\text{Sr}$ of both adult and young specimens. The third molar has a $\delta^{88}\text{Sr}$ value of -0.26 ‰, which is significantly higher than first molars and deciduous teeth. These results are shown in Fig. 2A according to the tooth eruption order in baboon life. The $^{87}\text{Sr}/^{86}\text{Sr}$ values for the ten baboon specimens are presented in Fig. 2B. There appears to be three significantly different clusters of specimens. Six specimens with high $^{87}\text{Sr}/^{86}\text{Sr}$ values (0.722 to 0.721), three adult females with low values (0.719) and one adult male with a very low value (0.716).

The $\delta^{88}\text{Sr}$ values and $^{87}\text{Sr}/^{86}\text{Sr}$ ratios of KNP and WC animals are given in Table S2 and shown in Fig. 3 according to species. They were all obtained using the LGLTPE-2 method. The $\delta^{88}\text{Sr}$ values range from -0.52 to -0.21 ‰ in enamel and from -0.28 to -0.02 ‰ in plant. At KNP, the mean $\delta^{88}\text{Sr}$ value for herbivores is -0.45 ± 0.17 ‰ (2SD, $n = 11$) and is -0.39 ± 0.07 ‰ (2SD, $n = 5$) for carnivores. At WC, there is one herbivorous specimen only (*Tragelaphus scriptus*) and its $\delta^{88}\text{Sr}$ value is -0.45 ‰, indistinguishable from the mean $\delta^{88}\text{Sr}$ value of *Panthera Leo*, which is -0.44 ± 0.10 ‰ (2SD, $n = 5$). The $^{87}\text{Sr}/^{86}\text{Sr}$ ratios range from 0.707 to 0.760 at KNP and from 0.709 to 0.730 at WC and are consistent with previous results (Balter et al., 2008). This variation range is important and can be explained by the complex geological context of these regions (Schutte, 1986; Shone and Booth, 2005).

4. Discussion

4.1. Strontium isotopes in reference materials

Despite small differences between the WIGL-UJ, LGLTPE-1 and LGLTPE-2 methods, notably in the chromatographic separation of Sr (Table 2) and the instrumental settings (Table 3), the $\delta^{88}\text{Sr}$ values of reference materials show excellent reproducibility between methods and very good accuracy when compared with literature values. This suggests that the overall protocol is robust, however several observations can be made for some analytical procedures. Consistent with the literature (Liu et al., 2012; Xu et al., 2020), the LGLTPE-2 method using the $^{92}\text{Zr}/^{90}\text{Zr}$ ratio to correct the instrumental mass bias on $^{88}\text{Sr}/^{86}\text{Sr}$ shows an enhanced accuracy with literature results (mean accuracy of 0.013 ‰ compared to (Krabbenhöft et al., 2009; Ma et al., 2013; Liu et al., 2017; Brazier et al., 2020)), than the LGLTPE-1 using $^{91}\text{Zr}/^{90}\text{Zr}$ ratio (mean

accuracy of 0.018 ‰ compared to (Krabbenhöft et al., 2009; Ma et al., 2013; Liu et al., 2017; Brazier et al., 2020)). The precision and accuracy at UJ (mean 2SD of 0.02 ‰, and mean accuracy of 0.015 ‰ compared to (Ma et al., 2013; Brazier et al., 2020)) are comparable to those achieved using LGLTPE-2 (mean 2SD of 0.04 ‰, and mean accuracy of 0.013 ‰), showing the importance of the on-peak baseline measurement with systematic blank subtraction. This was not done using LGLTPE-1 and clearly improves the precision of the results and lower the instrumental uncertainties ($U(k=2) = 0.09$ ‰ for LGLTPE-1 vs $U(k=2) = 0.04$ ‰ for LGLTPE-2 and UJ). The present results agree very well with the literature, which highlights a clear offset towards ^{88}Sr -depleted biological materials originating from animals (Brazier et al., 2020). To the best of our knowledge, three reference materials studied here had not been analyzed for strontium isotopes. The SRM-915b is a calcium carbonate standard used in analyses of Ca stable isotopes. It has been measured in three different aliquots, and the mean of its $^{87}\text{Sr}/^{86}\text{Sr}$ ratio is 0.70800 ± 0.00005 (2SD, $n = 3$). The mean $\delta^{88}\text{Sr}$ value is 0.33 ± 0.01 ‰ (2SD, $n = 2$) using the LGLTPE-1 method and 0.21 ‰ using the LGLTPE-2 method. Further measurements are needed to resolve this discrepancy, but we emphasize that the LGLTPE-2 mean is most probably closer to the true value. The NBS-120c is a phosphorite rock, which has been measured in three different aliquots yielding a mean $^{87}\text{Sr}/^{86}\text{Sr}$ ratio of 0.70885 ± 0.00005 (2SD, $n = 3$) and a mean $\delta^{88}\text{Sr}$ value of 0.41 ± 0.06 ‰ (2SD, $n = 3$). Once again, the dispersion between LGLTPE-1 and LGLTPE-2 is quite high. It must be noted that this material shows the highest $\delta^{88}\text{Sr}$ value measured in this study. It may be linked with its phosphate nature. Granite GA is a geochemical reference sample of granite material. It has been measured in three different aliquots, yielding a mean $^{87}\text{Sr}/^{86}\text{Sr}$ ratio of 0.71376 ± 0.00005 (2SD, $n = 3$). The mean $\delta^{88}\text{Sr}$ value measured using LGLTPE-1 is 0.33 ± 0.04 ‰ (2SD, $n = 2$) and the one measured using LGLTPE-2 is 0.22 ± 0.03 ‰. Further measurements are needed to choose between these two values, but the LGLTPE-2 mean is most probably closer to the actual value. As the measurement method is shown to be reliable using reference materials, it is possible to interpret the results obtained on biological material such as plant and tooth enamel.

4.2. Intra-individual variations of enamel Sr isotopes

The study of different tooth types in modern baboons allows evaluation of the extent of intra-individual variations of the $\delta^{88}\text{Sr}$ value. Of note is that all the baboon teeth have negative $\delta^{88}\text{Sr}$ values, in accordance with available data for bone and teeth (Knudson et al., 2010; Romaniello et al., 2015; Lewis et al., 2017; Brazier et al., 2020). Discussion on the possible use of the $\delta^{88}\text{Sr}$ value as a dietary proxy is challenging for baboons because there is a lack of isotopic data for possible dietary sources, which could be numerous as these are omnivorous animals (Hamilton III et al., 1978; Codron et al., 2006; Johnson et al., 2013). The most obvious pattern is a clear difference between the $\delta^{88}\text{Sr}$ value of milk and permanent teeth, the latter being ^{88}Sr -enriched compared to the former. This indicates a difference of diet between baboons older than six years old and baboons younger than four. The most likely explanation is that young baboons consume breast milk in various but decreasing amounts during their first years. It is known that the Sr/Ca ratio is much lower in breast milk than in other non-milk foods (Sillen and Smith, 1984; Mays, 2003; Humphrey et al., 2008; Nava et al., 2020). This difference between milk and non-milk food is explained by bio-purification processes, discriminating Sr against Ca in the mother's body. For instance, Ca is preferentially transferred across the mammary gland during lactation, whereas the circulation of Sr is passively constrained by the concentration gradient (Tsutaya and Yoneda, 2015). This process is known to also induce a mass-dependent fractionation of Ca isotopes, where milk is ^{44}Ca -depleted. The resulting negative $\delta^{44/42}\text{Ca}$ signature and lower Sr/Ca ratio is found in human deciduous teeth and yields information about lactation period and weaning processes in modern and ancient human population (Tacail et al., 2017, 2019; Li

et al., 2020).

The present $\delta^{88}\text{Sr}$ results suggest that Sr isotopes may also undergo mass-fractionation through mammary glands leading to a ^{88}Sr -depleted breast milk, compared to non-milk food and can trace the intensity of breast feeding and duration of the weaning process. Defining $\Delta^{88}\text{Sr}_t$ for one individual as the difference between the $\delta^{88}\text{Sr}$ value in the first molar and another tooth, shows decreasing values with increasing age at tooth eruption (Fig. 2A). Providing that milk has a low $\delta^{88}\text{Sr}$ value, this suggests the declining contribution of milk in baboon's diet as the animal ages. More precisely, during the first two-to-three months of life, young baboons are mostly breastfed and start to include non-milk food after the fourth month, while continuing to consume mother's milk to some extent. After the first year, baboons seem to shift to a milk-free adult diet. These dietary histories are consistent with known weaning processes of baboons (Rhine et al., 1985; Humphrey et al., 2008).

The $^{87}\text{Sr}/^{86}\text{Sr}$ ratios have been measured in the first molars and are distributed according to three groups (Fig. 2B) that should represent distinct bedrock types of the WC region. The $^{87}\text{Sr}/^{86}\text{Sr}$ ratios measured in enamel are consistent with the variability of the bioavailable $^{87}\text{Sr}/^{86}\text{Sr}$ ratios of plants measured in this area. In this region, the plant $^{87}\text{Sr}/^{86}\text{Sr}$ value gradually increases from 0.7087 to 0.7242 over 100 km between the coast and the land (Copeland et al., 2016). The baboons $^{87}\text{Sr}/^{86}\text{Sr}$ values thus indicate that the specimens were not living altogether at the same place when their first molars were forming. The baboons analyzed here originated from two different troops that were killed during hunting for population control in the Calitzdorp area (Brand, 1994). Chacma baboons are known to form sub-troops seasonally (Anderson, 1981), which are composed of a majority of adult females and young baboons (Anderson, 1981; Busse, 1984; Henzi et al., 1999). While it is not possible to reallocate baboon individuals in one or the other troop, our results however suggest that the $^{87}\text{Sr}/^{86}\text{Sr}$ ratio in enamel can help to reconstitute sub-trooping recruitment strategies in living primates.

4.3. Inter-individual variations of enamel Sr isotopes

For individuals found with plant residues, a $\Delta^{88}\text{Sr}_d$ can be defined as the difference between $\delta^{88}\text{Sr}$ value of the animal and that of the plant (Fig. 3). TM16661-PR and TM16690-PR are plant residues from teeth of specimens that were not analyzed in this study. The $\Delta^{88}\text{Sr}_d$ is always negative, indicating that the $\delta^{88}\text{Sr}$ values of herbivores tooth enamel is ^{88}Sr -depleted relative to plants, consistent with a feeding study performed on pigs (Lewis et al., 2017). These authors found a $\Delta^{88}\text{Sr}_d$ value of -0.32 ± 0.06 ‰, close to the average of -0.26 ‰ calculated here. Our results exhibit a much higher dispersion of the $\Delta^{88}\text{Sr}_d$ values, which can be explained by the natural, and therefore uncontrolled, context of the study. A Wilcoxon rank test was performed on all the $\delta^{88}\text{Sr}$ dataset of KNP to compare results for herbivores and carnivores. The P-value obtained is 0.03 suggesting that the differences between herbivores and carnivores can be considered significant. Thus, the $\Delta^{88}\text{Sr}_d$ values can also be calculated from enamel of carnivores to herbivores, and are, strikingly, not negative. At KNP, the $\Delta^{88}\text{Sr}_d$ value is 0.06 ‰, but it reaches 0.08 ‰ when one possible herbivore outlier (*Sylvicapra grimmia*) is excluded. Indeed, *Sylvicapra grimmia* presents the highest $\delta^{88}\text{Sr}$ and $^{87}\text{Sr}/^{86}\text{Sr}$ values (respectively -0.21 ‰ and 0.760) in the KNP dataset, which suggests a location effect. *Equus burchelli* also presents a higher $\delta^{88}\text{Sr}$ value than the other herbivores and represents the only pure grazer in the herbivore set, so different metabolisms may play a role in $\delta^{88}\text{Sr}$ differences. In the WC, the $\Delta^{88}\text{Sr}_d$ value is 0.01 ‰, but it is a less robust measure due to the presence of only one herbivore. The pattern of the Sr stable isotopes fractionation from plants to carnivores resembles that of Zn, for which the $\delta^{66}\text{Zn}$ value first strongly increases from plants to herbivores and then decreases to carnivores (Jaouen et al., 2013). The systematics of Sr stable isotope fractionation up mammal trophic chain thus requires further investigations to understand the origin of the observed isotopic variability before validating the $\delta^{88}\text{Sr}$ value as a robust

proxy of past diet and trophic position.

4.4. Further perspectives for combined stable and radiogenic Sr analyses

The present study emphasizes the interest and feasibility of analyzing the $\delta^{88}\text{Sr}$ and $^{87}\text{Sr}/^{86}\text{Sr}$ values simultaneously. Cost and duration of measurement is the same as when analyzing one or the other independently using MC-ICP-MS. The Sr chromatographic separation for 24 samples takes a day only, and with the whole SSB procedure, one sample can be analyzed in 45 min. The simplicity of the methodology will surely encourage more studies using stable and radiogenic Sr isotopes for (paleo)ecological and geological purposes.

Other non-traditional stable isotopes are already fulfilling the role of dietary/weaning tracer, such as $\delta^{44/42}\text{Ca}$ (Martin et al., 2018; Tacail et al., 2019, 2020, 2021), and $\delta^{66/64}\text{Zn}$ (Jaouen et al., 2013, 2016, 2020; Bourgon et al., 2020) measured in the mineral phase (hydroxyapatite) of bone and teeth. So far, the original $\delta^{44/42}\text{Ca}$ and $\delta^{66/64}\text{Zn}$ signatures are shown to be preserved in tooth enamel hydroxyapatite, (Martin et al., 2015; Hassler et al., 2018; Bourgon et al., 2020). As presented here, the combined $\delta^{88}\text{Sr}$ and $^{87}\text{Sr}/^{86}\text{Sr}$ analyses in animal and vegetal tissues provide information about diet and localization, and thus may enable an extended reconstruction of life history. Further work is needed to assess the preservation of the biological signature of Sr isotopes in fossil bone and tooth enamel. More studies are also needed to decipher the behavior of Sr through metabolic processes such as digestion or milk production, because metabolism may override the Sr dietary isotopic signature. The $\delta^{88}\text{Sr}$ value could represent a metabolic signature of the studied taxa. Results of stable Sr isotopes have been recently obtained by Nitzsche et al. in invertebrates of a stream food web (Nitzsche et al., 2022). The $\delta^{88}\text{Sr}$ value seems to discriminate different feeding behaviors and might be a dietary tracer in aquatic as well as terrestrial ecosystems.

The perspectives of $\delta^{88}\text{Sr}$ and $^{87}\text{Sr}/^{86}\text{Sr}$ combined analyses are not restricted to paleo(ecological) studies. A temperature dependent Sr isotope fractionation occurs between water and biologically mineralized carbonates. A $0.033\text{‰}/^\circ\text{C}$ thermodependency is reported for natural coral samples (*Pavona clavus*) (Fietzke and Eisenhauer, 2006) and a similar value of $0.026\text{‰}/^\circ\text{C}$ has been determined for another coral species (*Lophelia pertusa*) (Rüggeberg et al., 2008). A preliminary study shows that there might be a similar thermo-dependent process of fractionation for stable Sr isotopes in coccolithophore species (Stevenson et al., 2014). These studies suggest that the $\delta^{88}\text{Sr}$ value in carbonates could be used as a paleothermometer to reconstruct ancient ocean temperatures along with the $^{87}\text{Sr}/^{86}\text{Sr}$ value that could be used as a time calibration tool (Veizer et al., 1999).

Considering the differences between silicate-dominated (Bulk silicate Earth $\delta^{88}\text{Sr}$ value estimated as 0.29‰ (Ma et al., 2013)) and carbonate-dominated systems (Marine carbonates $\delta^{88}\text{Sr}$ value between 0.10 and 0.20‰ (Krabbenhöft et al., 2010)), the measurement of $\delta^{88}\text{Sr}$ could be an added value to that of $^{87}\text{Sr}/^{86}\text{Sr}$ for studying weathering processes. There is a preferential leaching of heavy Sr isotopes into the hydrosphere during silicate weathering, but a preferential leaching of light Sr isotope preferential leaching of heavy strontium during primary formed carbonate weathering (Chao et al., 2015). The river $\delta^{88}\text{Sr}$ value is therefore different whether it is carbonate- or silicate-dominated and this helps to identify the weathering processes that occurred before the water reached the river. The concomitant analysis of the $^{87}\text{Sr}/^{86}\text{Sr}$ value could give additional constrains on the provenance of the weathered material.

5. Conclusion

The measurement of Sr stable isotopes by MC-ICPMS using combined sample-standard bracketing and Zr correction is shown to be a robust and easy method. The method permits the simultaneous measurement of the stable $^{88}\text{Sr}/^{86}\text{Sr}$ and radiogenic $^{87}\text{Sr}/^{86}\text{Sr}$ ratios. This method has been implemented and evaluated in different laboratories and yields

accurate and reproducible results on a wide variety of reference materials. Preliminary results on tooth enamel samples show that the $\delta^{88}\text{Sr}$ value is a potential indicator of weaning practices. Encouraging results show that enamel $\delta^{88}\text{Sr}$ values potentially discriminate herbivores from carnivores, but this necessitates further studies to understand the source of isotopic heterogeneity. Generally, more data is necessary to better understand the effect of physiology on Sr isotopes and to extend the use of the $\delta^{88}\text{Sr}$ values as a companion of $\delta^{44/42}\text{Ca}$ in biomedical studies.

Declaration of Competing Interest

There are no conflicts of interest to declare.

Acknowledgements

Many thanks are due to the Ditsong National Museum of Natural History (Pretoria, South Africa), for providing access to the samples. We would like to thank Clément P. Bataille, and an anonymous reviewer for their helpful comments that helped improve the clarity of the paper.

Appendix A. Supplementary data

Supplementary materials are available for this article and include Tables S1, S2, S3, S4, S5, and Figs. S1, S2 and S3. Supplementary data to this article can be found online at <https://doi.org/10.1016/j.chemgeo.2022.121000>.

References

- Anderson, C.M., 1981. Subgrouping in a chacma baboon (*Papio ursinus*) population. *Primates* 22, 445–458.
- Argentino, C., Lugli, F., Cipriani, A., Panieri, G., 2021. Testing miniaturized extraction chromatography protocols for combined $^{87}\text{Sr}/^{86}\text{Sr}$ and $^{88}\text{Sr}/^{86}\text{Sr}$ analyses of pore water by MC-ICP-MS. *Limnol. Oceanogr. Methods* 19, 431–440.
- Balter, V., 2004. Allometric constraints on Sr/cr and Ba/cr partitioning in terrestrial mammalian trophic chains. *Oecologia* 139, 83–88.
- Balter, V., Telouk, P., Reynard, B., Braga, J., Thackeray, F., Albarède, F., 2008. Analysis of coupled Sr/cr and $^{87}\text{Sr}/^{86}\text{Sr}$ variations in enamel using laser-ablation tandem quadrupole-multicollector ICPMS. *Geochim. Cosmochim. Acta* 72, 3980–3990.
- Bourgon, N., Jaouen, K., Bacon, A.-M., Jochum, K.P., Dufour, E., Düringer, P., Ponche, J.-L., Joannes-Boyau, R., Boesch, Q., Antoine, P.-O., others, 2020. Zinc isotopes in late Pleistocene fossil teeth from a Southeast Asian cave setting preserve paleodietary information. *Proc. Natl. Acad. Sci.* 117, 4675–4681.
- Brand, D., 1994. Weight growth of chacma baboons in the southern Cape province, South Africa. *Rev. Zool. Afr.* 108, 71–75.
- Brazier, J.-M., Schmitt, A.-D., Pelt, E., Lemarchand, D., Gangloff, S., Tacail, T., Balter, V., 2020. Determination of radiogenic $^{87}\text{Sr}/^{86}\text{Sr}$ and stable $^{88}\text{Sr}/^{86}\text{Sr}$ isotope values of thirteen mineral, vegetal and animal reference materials by DS-TIMS. *Geostand. Geoanal. Res.* 44 (2), 331–348. <https://doi.org/10.1111/ggr.12308>.
- Busse, C.D., 1984. Spatial structure of chacma baboon groups. *Int. J. Primatol.* 5, 247–261.
- Chao, H.-C., You, C.-F., Liu, H.-C., Chung, C.-H., 2015. Evidence for stable Sr isotope fractionation by silicate weathering in a small sedimentary watershed in southwestern Taiwan. *Geochim. Cosmochim. Acta* 165, 324–341.
- Charlier, B., Parkinson, I., Burton, K., Grady, M., Wilson, C., Smith, E., 2017. Stable strontium isotopic heterogeneity in the solar system from double-spike data. *Geochim. Perspect. Lett.* 4, 35–40.
- Codron, D., Lee-Thorp, J.A., Sponheimer, M., de Ruiter, D., Codron, J., 2006. Inter- and intrahabitat dietary variability of chacma baboons (*Papio ursinus*) in South African savannas based on fecal $\delta^{13}\text{C}$, $\delta^{15}\text{N}$, and $\delta^{88}\text{Sr}$. *Am. J. Phys. Anthropol. Off. Publ. Am. Assoc. Phys. Anthropol.* 129, 204–214.
- Copeland, S.R., Cawthra, H.C., Fisher, E.C., Lee-Thorp, J.A., Cowling, R.M., Le Roux, P.J., Hodgkins, J., Marean, C.W., 2016. Strontium isotope investigation of ungulate movement patterns on the Pleistocene Paleo-Agulhas plain of the Greater Cape floristic region, South Africa. *Quat. Sci. Rev.* 141, 65–84.
- De Muynck, D., Huelga-Suarez, G., Van Heghe, L., Degryse, P., Vanhaecke, F., 2009. Systematic evaluation of a strontium-specific extraction chromatographic resin for obtaining a purified Sr fraction with quantitative recovery from complex and Ca-rich matrices. *J. Anal. At. Spectrom.* 24, 1498–1510.
- Ehrlich, S., Gavrieli, I., Dor, L.-B., Halicz, L., 2001. Direct high-precision measurements of the $^{87}\text{Sr}/^{86}\text{Sr}$ isotope ratio in natural water, carbonates and related materials by multiple collector inductively coupled plasma mass spectrometry (MC-ICP-MS). *J. Anal. At. Spectrom.* 16, 1389–1392.
- Fietzke, J., Eisenhauer, A., 2006. Determination of temperature-dependent stable strontium isotope ($^{88}\text{Sr}/^{86}\text{Sr}$) fractionation via bracketing standard MC-ICP-MS. *Geochim. Geophys. Geosyst.* 7.

- Guibourdenche, L., Stevenson, R., Pedneault, K., Poirier, A., Widory, D., 2020. Characterizing nutrient pathways in Quebec (Canada) vineyards: Insight from stable and radiogenic strontium isotopes. *Chem. Geol.* 532, 119375.
- Hajj, F., Poszwa, A., Bouchez, J., Guérol, F., 2017. Radiogenic and “stable” strontium isotopes in provenance studies: a review and first results on archaeological wood from shipwrecks. *J. Archaeol. Sci.* 86, 24–49.
- Hamilton III, W.J., Buskirk, R.E., Buskirk, W.H., 1978. Omnivory and utilization of food resources by chacma baboons, *Papio ursinus*. *Am. Nat.* 112, 911–924.
- Hassler, A., Martin, J.E., Amiot, R., Tacaïl, T., Godet, F.A., Allain, R., Balter, V., 2018. Calcium isotopes offer clues on resource partitioning among cretaceous predatory dinosaurs. *Proc. R. Soc. B Biol. Sci.* 285, 20180197.
- Henzi, S., Weingrill, T., Barrett, L., 1999. Male behaviour and the evolutionary ecology of chacma baboons. *South Afr. J. Sci.* 95, 240–242.
- Humphrey, L.T., Dirks, W., Dean, M.C., Jeffries, T.E., 2008. Tracking dietary transitions in weanling baboons (*Papio hamadryas anubis*) using strontium/calcium ratios in enamel. *Folia Primatol. (Basel)* 79, 197–212.
- Irrgeher, J., Prohaska, T., Sturgeon, R.E., Mester, Z., Yang, L., 2013. Determination of strontium isotope amount ratios in biological tissues using MC-ICPMS. *Anal. Methods* 5, 1687–1694.
- Jaouen, K., Pons, M.-L., Balter, V., 2013. Iron, copper and zinc isotopic fractionation up mammal trophic chains. *Earth Planet. Sci. Lett.* 374, 164–172.
- Jaouen, K., Beasley, M., Schoeninger, M., Hublin, J.-J., Richards, M.P., 2016. Zinc isotope ratios of bones and teeth as new dietary indicators: results from a modern food web (Koobi Fora, Kenya). *Sci. Rep.* 6, 26281.
- Jaouen, K., Trost, M., Bourgon, N., Colleter, R., Le Cabec, A., Tütken, T., Elias, Oliveira R., Pons, M.L., Méjean, P., Steinbrenner, S., others, 2020. Zinc isotope variations in archaeological human teeth (Lapa do Santo, Brazil) reveal dietary transitions in childhood and no contamination from gloves. *PLoS One* 15, e0232379.
- Johnson, C.A., Raubenheimer, D., Rothman, J.M., Clarke, D., Swedell, L., 2013. 30 days in the life: daily nutrient balancing in a wild chacma baboon. *PLoS One* 8.
- Knudson, K.J., Price, T.D., Buikstra, J.E., Blom, D.E., 2004. The use of strontium isotope analysis to investigate Tiwanaku migration and mortuary ritual in Bolivia and Peru. *Archaeometry* 46, 5–18.
- Knudson, K.J., Williams, H.M., Buikstra, J.E., Tomczak, P.D., Gordon, G.W., Anbar, A.D., 2010. Introducing $^{88}\text{Sr}/^{86}\text{Sr}$ analysis in archaeology: a demonstration of the utility of strontium isotope fractionation in paleodietary studies. *J. Archaeol. Sci.* 37, 2352–2364.
- Krabbenhöft, A., Fietzke, J., Eisenhauer, A., Liebetrau, V., Böhm, F., Vollstaedt, H., 2009. Determination of radiogenic and stable strontium isotope ratios ($^{87}\text{Sr}/^{86}\text{Sr}$; $\delta^{88}\text{Sr}/^{86}\text{Sr}$) by thermal ionization mass spectrometry applying an $^{87}\text{Sr}/^{84}\text{Sr}$ double spike. *J. Anal. At. Spectrom.* 24, 1267–1271.
- Krabbenhöft, A., Eisenhauer, A., Böhm, F., Vollstaedt, H., Fietzke, J., Liebetrau, V., Augustin, N., Peucker-Ehrenbrink, B., Müller, M., Horn, C., others, 2010. Constraining the marine strontium budget with natural strontium isotope fractionations ($^{87}\text{Sr}/^{86}\text{Sr}$, $^{88}\text{Sr}/^{86}\text{Sr}$) of carbonates, hydrothermal solutions and river waters. *Geochim. Cosmochim. Acta* 74, 4097–4109.
- Lazzzerini, N., Balter, V., Coulon, A., Tacaïl, T., Marchina, C., Lemoine, M., Bayarkhuu, N., Turbat, T., Lepetz, S., Zazzo, A., 2021. Monthly mobility inferred from isoscapes and laser ablation strontium isotope ratios in caprine tooth enamel. *Sci. Rep.* 11, 2277.
- Lewis, J., Pike, A., Coath, C., Evershed, R., 2017. Strontium concentration, radiogenic ($^{87}\text{Sr}/^{86}\text{Sr}$) and stable ($\delta^{88}\text{Sr}$) strontium isotope systematics in a controlled feeding study. *STAR Sci. Technol. Archaeol. Res.* 3, 45–57.
- Li, Q., Nava, A., Reynard, L.M., Thirlwall, M., Bondioli, L., Müller, W., 2020. Spatially-resolved Ca isotopic and trace element variations in human deciduous teeth record diet and physiological change. *Environ. Archaeol.* 1–10.
- Liu, H.-C., You, C.-F., Huang, K.-F., Chung, C.-H., 2012. Precise determination of triple Sr isotopes ($^{87}\text{Sr}/^{86}\text{Sr}$ and ^{88}Sr) using MC-ICP-MS. *Talanta* 88, 338–344.
- Liu, H.-C., Chung, C.-H., You, C.-F., Chiang, Y.-H., 2016. Determination of $^{87}\text{Sr}/^{86}\text{Sr}$ and $\delta^{88}\text{Sr}/^{86}\text{Sr}$ ratios in plant materials using MC-ICP-MS. *Anal. Bioanal. Chem.* 408, 387–397.
- Liu, H.-C., You, C.-F., Zhou, H., Huang, K.-F., Chung, C.-H., Huang, W.-J., Tang, J., 2017. Effect of calcite precipitation on stable strontium isotopic compositions: insights from riverine and pool waters in a karst cave. *Chem. Geol.* 456, 85–97.
- Ma, J., Wei, G., Liu, Y., Ren, Z., Xu, Y., Yang, Y., 2013. Precise measurement of stable ($\delta^{88}\text{Sr}/^{86}\text{Sr}$) and radiogenic ($^{87}\text{Sr}/^{86}\text{Sr}$) strontium isotope ratios in geological standard reference materials using MC-ICP-MS. *Chin. Sci. Bull.* 58, 3111–3118.
- Maréchal, C.N., Télouk, P., Albarède, F., 1999. Precise analysis of copper and zinc isotopic compositions by plasma-source mass spectrometry. *Chem. Geol.* 156, 251–273.
- Marisa Almeida, C., D. Vasconcelos, M.T.S., 2001. ICP-MS determination of strontium isotope ratio in wine in order to be used as a fingerprint of its regional origin. *J. Anal. At. Spectrom.* 16, 607–611.
- Martin, J.E., Tacaïl, T., Adnet, S., Girard, C., Balter, V., 2015. Calcium isotopes reveal the trophic position of extant and fossil elasmobranchs. *Chem. Geol.* 415, 118–125.
- Martin, J.E., Tacaïl, T., Cerling, T.E., Balter, V., 2018. Calcium isotopes in enamel of modern and Plio-Pleistocene East African mammals. *Earth Planet. Sci. Lett.* 503, 227–235. <https://doi.org/10.1016/j.epsl.2018.09.026>. ISSN 0012-821X.
- Mays, S., 2003. Bone strontium: calcium ratios and duration of breastfeeding in a Mediaeval skeletal population. *J. Archaeol. Sci.* 30, 731–741.
- McArthur, J.M., Howarth, R.J., Bailey, T.R., 2001. Strontium isotope stratigraphy: LOWESS version 3: best fit to the marine Sr-isotope curve for 0–509 Ma and accompanying look-up table for deriving numerical age. *J. Geol.* 109, 155–170. <https://doi.org/10.1086/319243>.
- Meija, J., Coplen, T.B., Berglund, M., Brand, W.A., De Bièvre, P., Gröning, M., Holden, N. E., Irrgeher, J., Loss, R.D., Walczyk, T., others, 2016. Atomic weights of the elements 2013 (IUPAC Technical Report). *Pure Appl. Chem.* 88, 265–291.
- Nava, A., Lugli, F., Romandini, M., Badino, F., Evans, D., Helbling, A.H., Oxilia, G., Arrighi, S., Bortolini, E., Delpiano, D., Duches, R., Figus, C., Livraghi, A., Marciari, G., Silvestrini, S., Cipriani, A., Giovanardi, T., Pini, R., Tuniz, C., Bernardini, F., Dori, I., Coppa, A., Cristiani, E., Dean, C., Bondioli, L., Peresani, M., Müller, W., Benazzi, S., 2020. Early life of Neanderthals. *Proc. Natl. Acad. Sci.* 117, 28719–28726.
- Neymark, L.A., Premo, W.R., Mel'nikov, N.N., Emsbo, P., 2014. Precise determination of $\delta^{88}\text{Sr}$ in rocks, minerals, and waters by double-spike TIMS: a powerful tool in the study of geological, hydrological and biological processes. *J. Anal. At. Spectrom.* 29, 65–75.
- Nitzsche, K.N., Wakaki, S., Yamashita, K., Shin, K.-C., Kato, Y., Kamauchi, H., Tayasu, I., 2022. Calcium and strontium stable isotopes reveal similar behaviors of essential Ca and nonessential Sr in stream food webs. *Ecosphere* 13, e3921.
- Ohno, T., Hirata, T., 2007. Simultaneous determination of mass-dependent isotopic fractionation and radiogenic isotope variation of strontium in geochemical samples by multiple collector-ICP-mass spectrometry. *Anal. Sci.* 23, 1275–1280.
- Price, T.D., Burton, J.H., Bentley, R.A., 2002. The characterization of biologically available strontium isotope ratios for the study of prehistoric migration. *Archaeometry* 44, 117–135.
- Rhine, R., Norton, G., Wynn, G., Wynn, R., 1985. Weaning of free-ranging infant baboons (*Papio cynocephalus*) as indicated by one-zero and instantaneous sampling of feeding. *Int. J. Primatol.* 6, 491.
- Romaniello, S., Field, M., Smith, H., Gordon, G., Kim, M., Anbar, A., 2015. Fully automated chromatographic purification of Sr and Ca for isotopic analysis. *J. Anal. At. Spectrom.* 30, 1906–1912.
- Rüggeberg, A., Fietzke, J., Liebetrau, V., Eisenhauer, A., Dullo, W.-C., Freiwald, A., 2008. Stable strontium isotopes ($^{88}\text{Sr}/^{86}\text{Sr}$) in cold-water corals—a new proxy for reconstruction of intermediate ocean water temperatures. *Earth Planet. Sci. Lett.* 269, 570–575.
- Russell, W., Papanastassiou, D., Tombrello, T., 1978. Ca isotope fractionation on the Earth and other solar system materials. *Geochim. Cosmochim. Acta* 42, 1075–1090.
- Schutte, I., 1986. The general geology of the Kruger National Park. *Koedoe Afr. Prot. Area Conserv. Sci.* 29, 13–37. <https://doi.org/10.4102/koedoe.v29i1.517>.
- Shone, R.W., Booth, P.W.K., 2005. The Cape Basin, South Africa: a review. *J. Afr. Earth Sci.* 43, 196–210.
- Sillen, A., Smith, P., 1984. Weaning patterns are reflected in strontium-calcium ratios of juvenile skeletons. *J. Archaeol. Sci.* 11, 237–245.
- Sillen, A., Balter, V., 2018. Strontium isotopic aspects of *Paranthropus robustus* teeth; implications for habitat, residence, and growth. *J. Human Evol.* 114, 118–130. <https://doi.org/10.1016/j.jhevol.2017.09.009>. ISSN 0047-2484.
- de Souza, G.F., Reynolds, B.C., Kiczka, M., Bourdon, B., 2010. Evidence for mass-dependent isotopic fractionation of strontium in a glaciated granitic watershed. *Geochim. Cosmochim. Acta* 74, 2596–2614.
- Stevenson, E.I., Hermalso, M., Rickaby, R.E., Tyler, J.J., Minoletti, F., Parkinson, I.J., Mokadem, J., Burton, K.W., 2014. Controls on stable strontium isotope fractionation in coccolithophores with implications for the marine Sr cycle. *Geochim. Cosmochim. Acta* 128, 225–235.
- Sullivan, K., Layton-Matthews, D., Leybourne, M., Kidder, J., Mester, Z., Yang, L., 2020. Copper Isotopic analysis in geological and biological reference materials by MC-ICP-MS. *Geostand. Geoanal. Res.* 44, 349–362.
- Tacaïl, T., Albalat, E., Télouk, P., Balter, V., 2014. A simplified protocol for measurement of Ca isotopes in biological samples. *J. Anal. At. Spectrom.* 29, 529–535.
- Tacaïl, T., Martin, J.E., Herrscher, E., Albalat, E., Verma, C., Ramirez-Rozzi, F., Clark, G., Valentin, F., Balter, V., 2021. Quantifying the evolution of animal dairy intake in humans using calcium isotopes. *Quant. Sci. Rev.* 256 (106843) <https://doi.org/10.1016/j.quascirev.2021.106843>. ISSN 0277-3791.
- Tacaïl, T., Thivichon-Prince, B., Martin, J.E., Charles, C., Viriot, L., Balter, V., 2017. Assessing human weaning practices with calcium isotopes in tooth enamel. *Proc. Natl. Acad. Sci.* 114, 6268–6273.
- Tacaïl, T., Le Houedec, S., Skulan, J.L., 2020. New frontiers in calcium stable isotope geochemistry: perspectives in present and past vertebrate biology. *Chem. Geol.* 537 (119471) <https://doi.org/10.1016/j.chemgeo.2020.119471>. ISSN 0009-2541.
- Tacaïl, T., Martin, J.E., Arnaud-Godet, F., Thackeray, J.F., Cerling, T.E., Braga, J., Balter, V., 2019. Calcium isotopic patterns in enamel reflect different nursing behaviors among South African early hominins. *Sci. Adv.* 5, eaax3250.
- Tsutaya, T., Yoneda, M., 2015. Reconstruction of breastfeeding and weaning practices using stable isotope and trace element analyses: a review. *Am. J. Phys. Anthropol.* 156, 2–21.
- Veizer, J., Ala, D., Azmy, K., Bruckschen, P., Buhl, D., Bruhn, F., Carden, G.A.F., Diener, A., Ebneth, S., Godderis, Y., Jasper, T., Korte, C., Pawellek, F., Podlaha, O.G., Strauss, H., 1999. $^{87}\text{Sr}/^{86}\text{Sr}$, $\delta^{13}\text{C}$ and $\delta^{18}\text{O}$ evolution of Phanerozoic seawater. *Chem. Geol.* 161, 59–88.
- Weber, M., Lugli, F., Jochum, K.P., Cipriani, A., Scholz, D., 2018. Calcium carbonate and phosphate reference materials for monitoring bulk and microanalytical determination of Sr isotopes. *Geostand. Geoanal. Res.* 42, 77–89.
- Xu, J., Yang, S., Yang, Y., Liu, Y., Xie, X., Spectroscopy, A., 2020. Precise determination of stable strontium isotopic compositions by MC-ICP-MS. *At. Spectrosc. Norwalk Conn.* 41, 64–73.